

Article

# Consideration of the Role of Plasma in a Plasma-Coupled Selective Catalytic Reduction of Nitrogen Oxides with a Hydrocarbon Reducing Agent

Byeong Ju Lee <sup>†</sup>, Ho-Chul Kang <sup>†</sup>, Jin Oh Jo and Young Sun Mok <sup>\*</sup> 

Department of Chemical and Biological Engineering, Jeju National University, Jeju 63243, Korea; qudwn211@jejunu.ac.kr (B.J.L.); khc0920@nate.com (H.-C.K.); zkfdh@jejunu.ac.kr (J.O.J.)

<sup>\*</sup> Correspondence: smokie@jejunu.ac.kr; Tel.: +82-64-754-3682; Fax: +82-64-755-3670

<sup>†</sup> Two authors contributed equally to this work.

Received: 13 October 2017; Accepted: 28 October 2017; Published: 31 October 2017

**Abstract:** The purpose of this study is to explain how plasma improves the performance of selective catalytic reduction (SCR) of nitrogen oxides (NO<sub>x</sub>) with a hydrocarbon reducing agent. In the plasma-coupled SCR process, NO<sub>x</sub> reduction was performed with n-heptane as a reducing agent over Ag/γ-Al<sub>2</sub>O<sub>3</sub> as a catalyst. We found that the plasma decomposes n-heptane into several oxygen-containing products such as acetaldehyde, propionaldehyde and butyraldehyde, which are more reactive than the parent molecule n-heptane in the SCR process. Separate sets of experiments using acetaldehyde, propionaldehyde and butyraldehyde, one by one, as a reductant in the absence of plasma, have clearly shown that the presence of these partially oxidized compounds greatly enhanced the NO<sub>x</sub> conversion. The higher the discharge voltage, the more the amounts of such partially oxidized products. The oxidative species produced by the plasma easily converted NO into NO<sub>2</sub>, but the increase of the NO<sub>2</sub> fraction was found to decrease the NO<sub>x</sub> conversion. Consequently, it can be concluded that the main role of plasma in the SCR process is to produce partially oxidized compounds (aldehydes), having better reducing power. The catalyst-alone NO<sub>x</sub> removal efficiency with n-heptane at 250 °C was measured to be less than 8%, but it increased to 99% in the presence of acetaldehyde at the same temperature. The NO<sub>x</sub> removal efficiency with the aldehyde reducing agent was higher as the number of carbons in the aldehyde was more; for example, the NO<sub>x</sub> removal efficiencies at 200 °C with butyraldehyde, propionaldehyde and acetaldehyde were measured to be 83.5%, 58.0% and 61.5%, respectively, which were far above the value (3%) obtained with n-heptane.

**Keywords:** selective catalytic reduction; plasma; nitrogen oxides; n-heptane; aldehydes

## 1. Introduction

Nitrogen oxides (NO<sub>x</sub>), together with volatile organic compounds (VOCs), are the main contributors to the generation of particulate matters or photochemical smog [1]. Although there are several conventional technologies for NO<sub>x</sub> removal, the ones based on catalysts are regarded as the most reliable and effective [2–5]. Generally, most of the catalysts used for the removal of NO<sub>x</sub> from exhaust gases have excellent activity at high temperatures of 250–450 °C [6–8], but the catalytic activity sharply decreases at lower temperatures. Up to now, many researchers have made great efforts to improve catalytic NO<sub>x</sub> reduction performances at low temperatures [9–12]. Particularly, when the temperature of exhaust gas fluctuates, it is very important to improve low-temperature catalytic activity to maintain a stable NO<sub>x</sub> reduction efficiency.

In order to improve the NO<sub>x</sub> reduction performance at low temperatures, a method of enhancing the reactivity in the catalyst by changing the NO/NO<sub>2</sub> ratio of the exhaust gas [11,12], or a method of improving the low-temperature catalytic activity by combining non-thermal plasma

with catalysis [9], have been studied by many researchers. It has been reported that adjusting the NO/NO<sub>2</sub> ratio to around 1/1 in ammonia selective catalytic reduction (NH<sub>3</sub>-SCR) results in the best catalytic activity, which is known as a fast selective catalytic reduction (SCR) reaction ( $\text{NO} + \text{NO}_2 + 2\text{NH}_3 \rightarrow 2\text{N}_2 + 3\text{H}_2\text{O}$ ) [13,14]. It has also been reported that increasing the NO<sub>2</sub> concentration in the hydrocarbon SCR (HC-SCR) improves the reactivity [15]. In the case of plasma-coupled catalytic processes, NO<sub>x</sub> can be more effectively removed by the oxidation of NO to NO<sub>2</sub> and partial oxidation of hydrocarbon [16,17].

A method of combining a plasma technique with a catalyst includes a one-stage method of generating plasma in a catalyst bed [17–20], and a two-stage configuration in which a catalytic reactor is installed downstream of the plasma reactor [16,21,22]. Jiang et al. [23] and Guan et al. [24] were able to effectively remove NO<sub>x</sub> using a two-stage reactor configuration in NH<sub>3</sub>-SCR. Besides, NO<sub>x</sub> was successfully removed over a wide range of temperatures with a high efficiency using a hydrocarbon as a reducing agent in a two-stage or one-stage reactor configuration [16,17,25]. In any case, it has been proven by many researchers that plasma could enhance the catalytic activity for NO<sub>x</sub> reduction, but it is still unclear how plasma promotes the catalytic reaction. It is understood that when the plasma is applied to the NH<sub>3</sub>-SCR, the oxidation of NO to NO<sub>2</sub> by plasma plays a key role in the enhancement of NO<sub>x</sub> removal, as already revealed in the fast SCR reaction [12,26]. However, in the case of HC-SCR, it is not clear why the plasma increases the catalytic reduction performance. Some researchers have interpreted that the formation of NO<sub>2</sub> by the oxidation of NO leads to an enhancement in NO<sub>x</sub> removal [16,17,27], and others explain the improvement of NO<sub>x</sub> reduction performance by the production of reactive intermediates from the decomposition of a hydrocarbon-reducing agent by plasma reforming [22,28].

In this study, systematic experiments have been conducted to understand the effect of plasma on the catalytic performance in HC-SCR and what mechanisms are involved in the enhancement of catalytic NO<sub>x</sub> reduction. The catalyst used in this work was gamma alumina-supported silver (Ag/γ-alumina). A one-stage plasma-catalytic reactor configuration has been employed so that the plasma could directly affect the catalyst. The NO<sub>x</sub> reducing agent used in this work was n-heptane (n-C<sub>7</sub>H<sub>16</sub>). First, in order to confirm the effect of NO<sub>2</sub> formation on the catalytic reaction, the NO/NO<sub>2</sub> ratio was artificially controlled, and its effect on the NO<sub>x</sub> removal rate was carefully examined. Another experiment was about the effect of hydrocarbon decomposition products on the catalytic reactions. The kinds of decomposition products produced when n-heptane is decomposed by plasma were analyzed. The identified decomposition products were used as reducing agents, one by one, to see whether the decomposition products actually increase the NO<sub>x</sub> removal performance, and if so, which decomposition product increases the NO<sub>x</sub> removal the most. Through such systematic experiments, we have tried to identify the mechanisms by which plasma increases NO<sub>x</sub> removal performance in the HC-SCR.

## 2. Results and Discussion

### 2.1. Plasma-Coupled SCR of NO<sub>x</sub>

The discharge powers determined at different voltages and temperatures are given in Figure 1a. As shown, the discharge power was mainly affected by the discharge voltage. Figure 1b shows the measured NO<sub>x</sub> conversions as a function of the applied voltage at several temperatures in the range of 100–250 °C, where the measurement at 0 kV indicates NO<sub>x</sub> removed only by the catalyst. As can be seen, the NO<sub>x</sub> conversion increased with increasing the voltage at all temperatures. Particularly, the higher the reactor temperature, the more rapid the increase of the NO<sub>x</sub> conversion rate as the voltage increased. These results show that the plasma affects the catalytic reaction in some way, and similar results have been obtained in many previous studies [21–27]. In Figure 1c, n-heptane consumptions at different voltages and temperatures are presented. The higher the reaction temperature and voltage were, the higher the n-heptane consumption was, which agrees well with Figure 1b. Figure 1d compares

the  $\text{NO}_x$  conversions of the plasma-coupled SCR with those of the SCR alone when the applied voltage was 25 kV. As shown in the figure, the  $\text{NO}_x$  conversion rate increased sharply by 30–80%, depending on whether plasma was generated in the catalyst bed or not. This result suggests that the plasma helps the catalyst to maintain its catalytic activity for  $\text{NO}_x$  reduction over a wide range of temperatures. Figure S1 shows a typical Fourier Transform Infrared (FTIR) spectrum of the effluent, where it can be observed that the main products from n-heptane were  $\text{CO}_2$  and  $\text{CO}$ . During the plasma-catalytic reaction, some part of  $\text{NO}_x$  was converted into nitrous oxide ( $\text{N}_2\text{O}$ ). The inset presents the concentration of nitrous oxide as a function of discharge voltage. The concentration of nitrous oxide increased from 16 to 29 ppm with increasing the voltage from 12 to 21 kV, and then decreased to 21 ppm at 25 kV.

In the case of  $\text{NH}_3$ -SCR, it is interpreted that the improvement of the catalytic activity by the plasma is attributed to the formation of  $\text{NO}_2$  by oxidation of  $\text{NO}$  [23,24]. Although the fact that plasma improves the performance of HC-SCR has been experimentally proven in many studies [16,17,22,27,29], the role of the plasma has not yet been clearly elucidated.

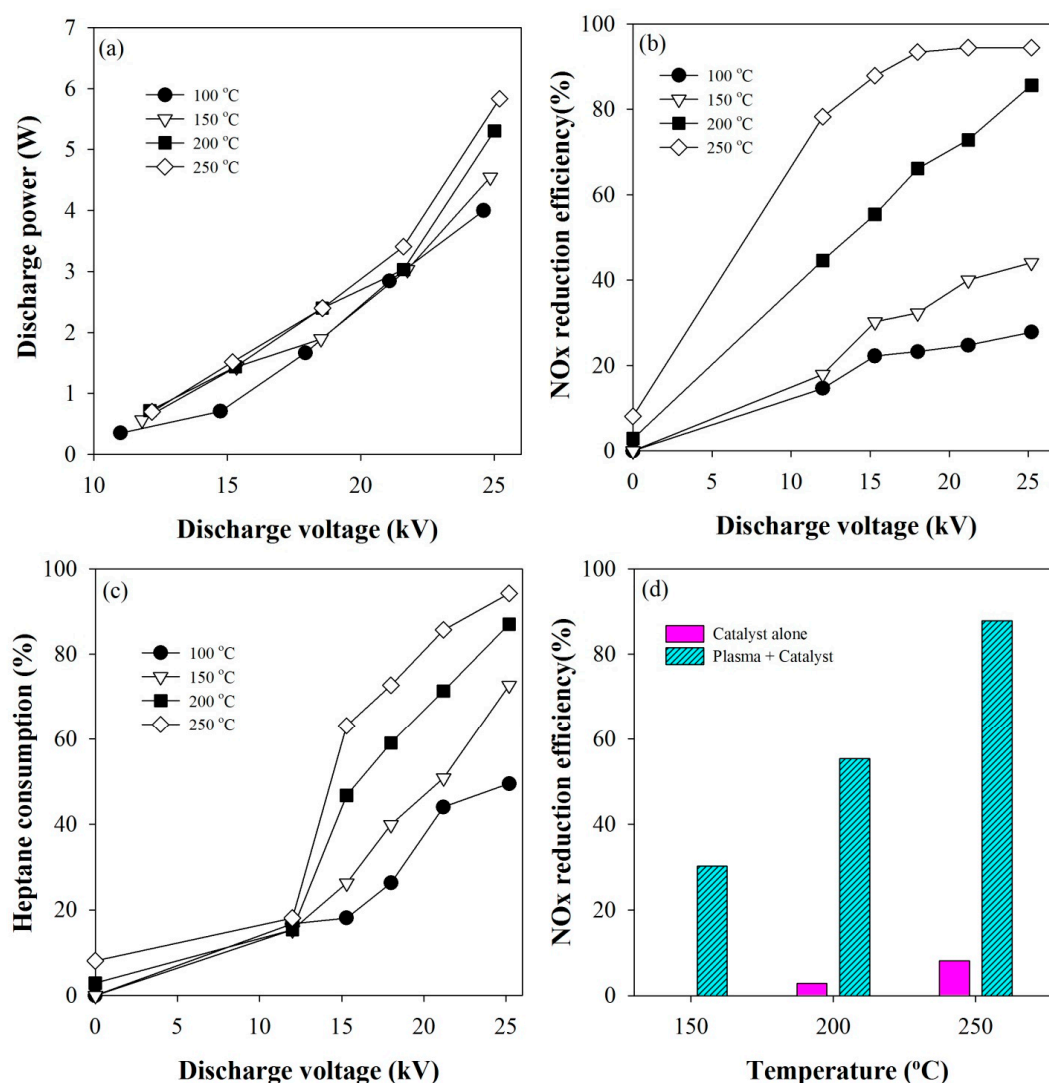


**Figure 1.** (a) Discharge powers at different voltages and temperatures; (b)  $\text{NO}_x$  conversions as a function of the applied voltage; (c) n-heptane consumption efficiencies at different voltages and temperatures; and (d) comparison of the  $\text{NO}_x$  conversions of the plasma-coupled HC-SCR with those of the HC-SCR alone.

## 2.2. Effect of NO<sub>2</sub> Fraction on the Catalytic Reduction of NO<sub>x</sub>

It was a matter of concern whether the formation of NO<sub>2</sub> in the HC-SCR enhances NO<sub>x</sub> reduction, as in the NH<sub>3</sub>-SCR. First, in order to clarify the effect of plasma generation on the oxidation of NO to NO<sub>2</sub>, several sets of experiments were carried out by filling bare  $\gamma$ -alumina in the quartz tube (i.e., without loading Ag). The feed consisted of NO 285 ppm and NO<sub>2</sub> 15 ppm. For these NO oxidation experiments, n-heptane, a reducing agent, was not injected. Figure S2 in the Supplementary Materials shows the outlet NO and NO<sub>2</sub> concentrations as a function of discharge voltage. As expected, as the voltage increased, NO decreased and NO<sub>2</sub> increased, but the total NO<sub>x</sub> (NO + NO<sub>2</sub>) remained almost constant. The increase in the NO oxidation rate when the voltage increased is, of course, because more oxidative active species were produced. The main reaction scheme for NO oxidation can be found in the literature [25]. Anyhow, ozone and O radicals generated by the plasma can easily oxidize NO to NO<sub>2</sub> as shown in the figure. Ozone is one of key oxidants produced by the plasma that can easily oxidize NO to NO<sub>2</sub>. Thus, tens to hundreds ppm of ozone generated by the plasma effectively increases the concentration of NO<sub>2</sub>. Ozone reacts with NO in a one to one stoichiometry, and the rate of reaction for the oxidation of NO to NO<sub>2</sub> is very fast (almost completed in a few tens of milliseconds) [30]. Thus, unless the discharge power is unreasonably high, ozone slip is negligible. The concentration of ozone is proportional to the applied voltage (discharge power). At unreasonably high discharge power, NO<sub>2</sub> can be further oxidized to NO<sub>3</sub> and N<sub>2</sub>O<sub>5</sub> [31,32]. Thus, the discharge power should be limited to avoid ozone slip and further oxidation of NO<sub>2</sub> to NO<sub>3</sub> and N<sub>2</sub>O<sub>5</sub>.

The following experiment was conducted to investigate the effect of NO<sub>2</sub> fraction in NO<sub>x</sub> on the NO<sub>x</sub> conversion. To investigate whether the NO<sub>x</sub> conversion rate really increases as the NO<sub>2</sub> fraction increases, as reported in the literature [16,17,27], catalytic NO<sub>x</sub> reduction was investigated by gradually increasing the NO<sub>2</sub> fraction. Figure 2a shows the NO<sub>x</sub> conversion according to the NO<sub>2</sub> fraction in NO<sub>x</sub>, and Figure 2b presents the concentrations of unreacted NO and NO<sub>2</sub>. The NO<sub>2</sub> fraction in the feed gas was varied in the range of 5–85% with keeping the NO<sub>x</sub> concentration at 300 ppm. The concentration of the reducing agent, n-heptane, was 257 ppm, which is equivalent to six times the NO<sub>x</sub> concentration on a C<sub>1</sub> basis. As shown in Figure 2a, as the NO<sub>2</sub> fraction increased, the NO<sub>x</sub> conversion tended to unexpectedly gradually decrease, implying that the increase in NO<sub>x</sub> conversion by the plasma in the HC-SCR is not due to the oxidation of NO to NO<sub>2</sub>. In the case of NH<sub>3</sub>-SCR, the oxidation of NO to NO<sub>2</sub> by the active components produced by plasma has been reported to have the greatest effect on the conversion rate improvement [23,24]. However, in HC-SCR, the cause of NO<sub>x</sub> conversion increase by plasma must be found elsewhere.

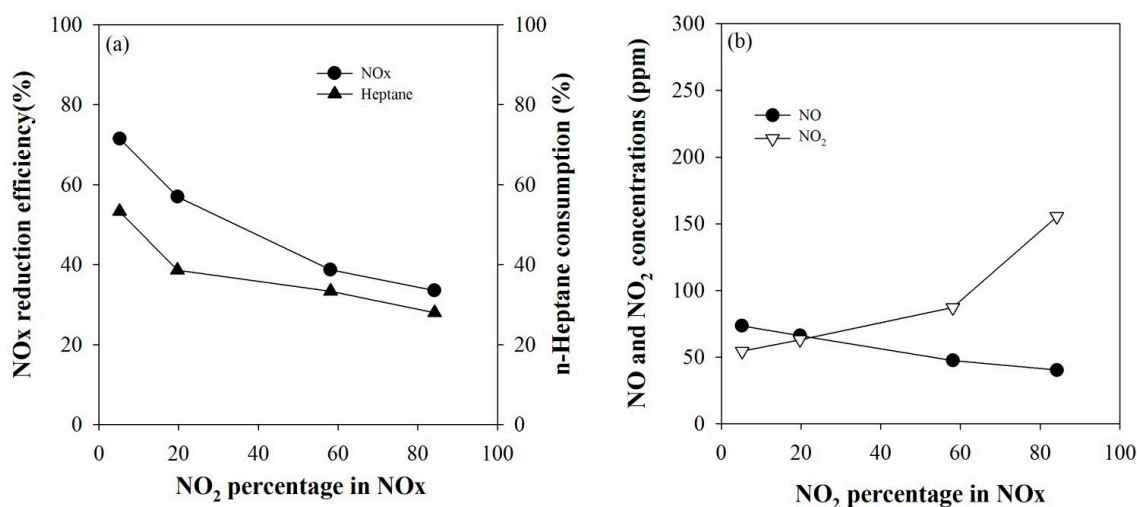


**Figure 2.** (a) Variations of the NO<sub>x</sub> conversions according to the NO<sub>2</sub> fraction in NO<sub>x</sub> and (b) concentrations of unreacted NO and NO<sub>2</sub>.

### 2.3. Effect of n-Heptane Decomposition Products on the Catalytic Reduction of $\text{NO}_x$

When n-heptane is decomposed by plasma, decomposition products may show better performance as a reducing agent than n-heptane itself. According to the literature [28,33], when the diesel fuel was reformed from the outside of the reactor using plasma and injected into the reactor as the reducing agent, the catalytic  $\text{NO}_x$  conversion was substantially improved. This increase of  $\text{NO}_x$  conversion was interpreted by the production of oxygenated hydrocarbons, such as aldehydes and alcohols, which are reformed products of diesel fuel [28]. In a similar vein, n-heptane, a reducing agent used in this study, can decompose in the plasma-SCR reactor into oxygenated hydrocarbons and improve  $\text{NO}_x$  conversion. First, gas chromatography and FTIR spectroscopy were used to identify what kinds of decomposition products were formed by plasma. Figure 3a shows the gas chromatography (GC) chromatogram obtained by injecting only n-heptane (257 ppm) into the reactor without injecting  $\text{NO}_x$  to see what decomposition products are formed by the plasma from n-heptane. According to the GC chromatogram obtained at 25 kV, major decomposition products of n-heptane were found to be oxygenated hydrocarbons, like acetaldehyde, propionaldehyde and butyraldehyde. Even though many unidentified low molecular weight hydrocarbons other than aldehydes were also produced as shown, the most abundant n-heptane decomposition products were such aldehydes. Figure S3 in the Supplementary Materials shows the concentrations of acetaldehyde, propionaldehyde and butyraldehyde as a function of discharge voltage. As is well-known, plasma-induced reactive species such as energetic electrons, radicals (O, OH, N) and ozone are involved in the formation of oxygenated hydrocarbons. It has been shown above that the increased  $\text{NO}_x$  conversion by plasma is not due to the formation of  $\text{NO}_2$ , which suggests that the decomposition products of n-heptane promote  $\text{NO}_x$  reduction reactions. Figure 3b shows the GC chromatogram obtained by injecting both n-heptane (257 ppm) and  $\text{NO}_x$  (300 ppm) into the reactor when the temperature was 250 °C. As seen, the aldehyde concentrations largely decreased, indicating that they were consumed by quickly reacting with  $\text{NO}_x$  on the catalyst surface.

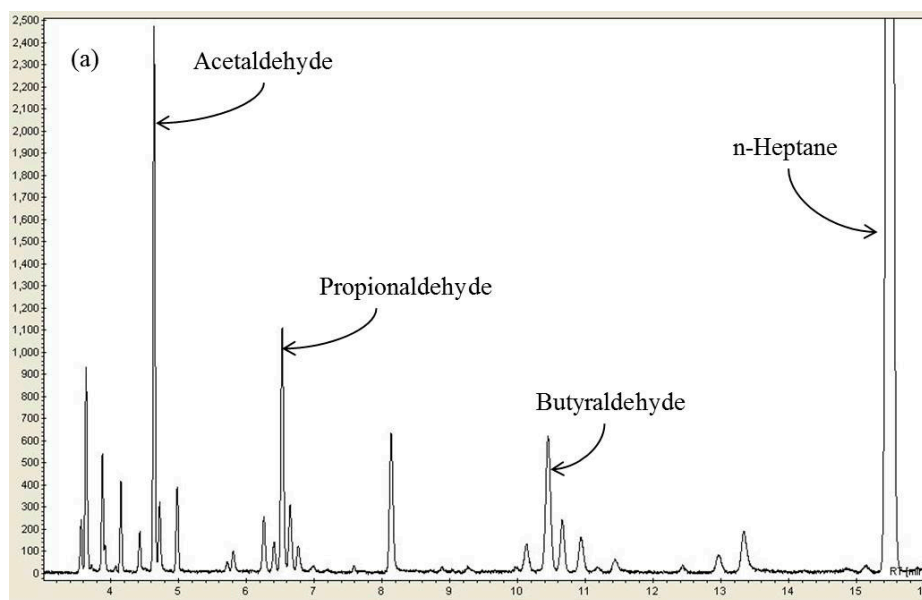
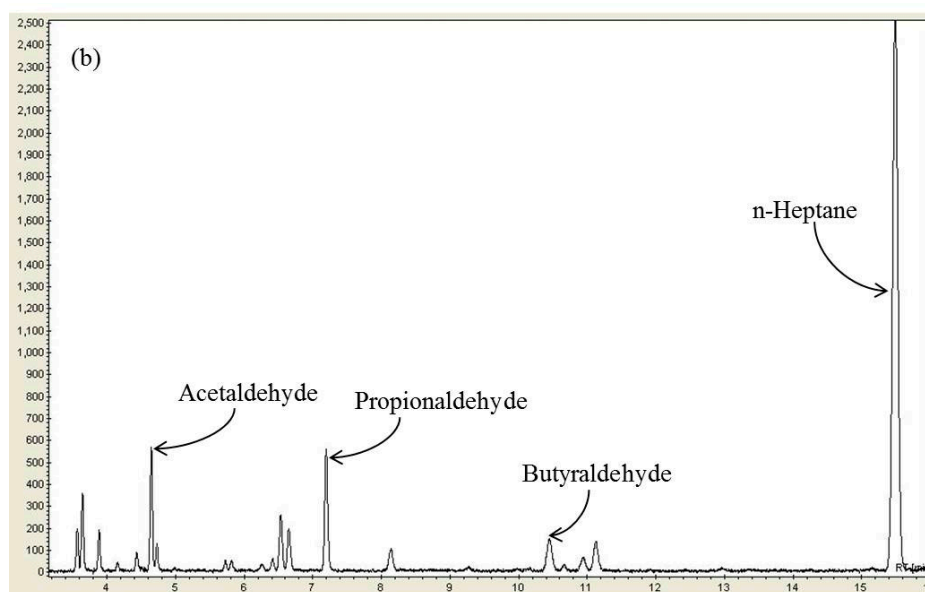
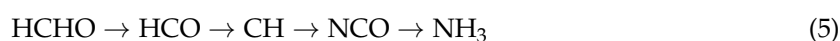
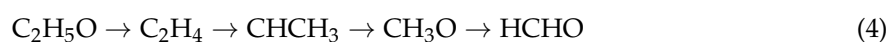


Figure 3. Cont.



**Figure 3.** (a) GC chromatogram of the n-heptane decomposition products and (b) GC chromatogram of the reaction products of n-heptane and NO<sub>x</sub> (n-heptane: 257 ppm; temperature: 250 °C; applied voltage: 25 kV).

In order to investigate whether aldehyde is effective at NO<sub>x</sub> conversion, several sets of catalyst-alone NO<sub>x</sub> removal experiments were carried out by injecting acetaldehyde, propionaldehyde and butyraldehyde, one by one, as a reducing agent. The concentration of each reducing agent was six times the NO<sub>x</sub> concentration on a C<sub>1</sub> basis. The experimental results are shown in Figure 4. As seen in the figure, acetaldehyde, propionaldehyde and butyraldehyde exhibited better NO<sub>x</sub> removal performance than the parent reducing agent n-heptane; the higher the molecular weight among the aldehydes, the higher the NO<sub>x</sub> conversion. This result clearly shows that the main role of plasma in the plasma-coupled HC-SCR process is to decompose hydrocarbons to produce degradation products with better reducing power than the parent hydrocarbon itself. As shown in Figure 3a, n-heptane decomposition produces such aldehydes. It is thought that the HC-SCR reaction proceeds with the decomposition reactions of hydrocarbon [15,34]. In order for n-heptane to serve as a reducing agent for NO<sub>x</sub> removal, it must first be decomposed through a series of complicated reaction steps. Since aldehydes are already in such a decomposed state, it is natural that NO<sub>x</sub> reduction performance should increase when an aldehyde is used as a reducing agent. It has been reported that the reactions taking place in HC-SCR involve the production of ammonia (NH<sub>3</sub>) via the formation of oxygenated hydrocarbons (C<sub>x</sub>H<sub>y</sub>O<sub>z</sub>) [34–36]. For example, alkanes (RH) produce aldehydes like CH<sub>3</sub>CHO through sequential oxidation reactions via alkoxy (RO) or alkyl (R) that are unstable intermediates, and aldehydes are eventually converted into NH<sub>3</sub> via isocyanate intermediate (NCO) on the catalyst surface [34]. For example, some of the pathways leading to NH<sub>3</sub> for the alkanes (C<sub>3</sub>–C<sub>10</sub>) are:



Once  $\text{NH}_3$  is formed, subsequent reactions are identical to those in  $\text{NH}_3$ -SCR:



When plasma is combined, aldehydes are formed by the decomposition of hydrocarbon, as discussed earlier. That is, since the step of converting the hydrocarbon to aldehydes is omitted, the above process can be performed more quickly in the presence of plasma. The concentration of  $\text{NH}_3$  measured at the reactor outlet was below the detection limit. Based on this result, it is considered that ammonia immediately reacts with  $\text{NO}_x$  as soon as it is formed via the Reactions (1)–(5).

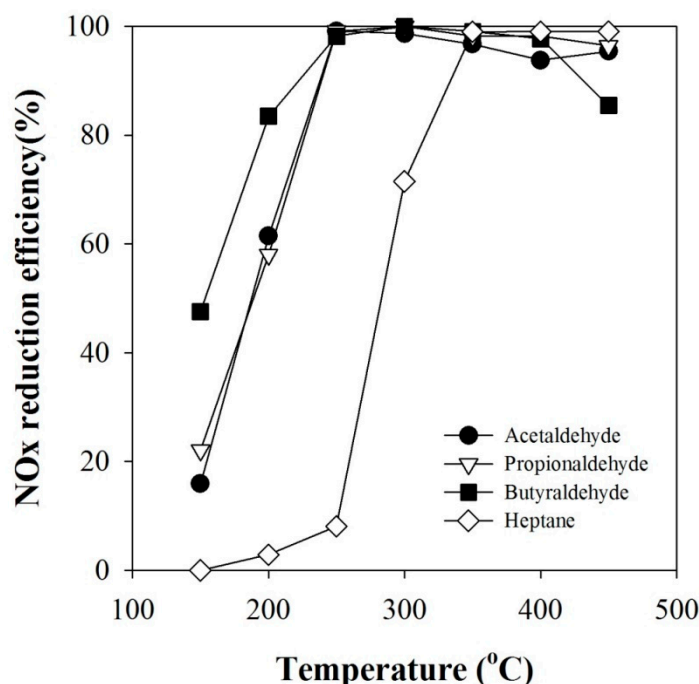


**Figure 4.** Catalyst-alone  $\text{NO}_x$  conversions obtained with n-heptane, acetaldehyde, propionaldehyde and butyraldehyde ( $\text{C}_1/\text{NO}_x$ : 6).

In relation to Figure 4, the concentrations of remaining aldehydes after the catalytic reactions without plasma are presented in Figure 5. As shown in the figure, the concentrations of the aldehydes decreased more rapidly than n-heptane. Among the aldehydes, the concentration of butyraldehyde decreased the fastest, followed by propionaldehyde and acetaldehyde, which shows a good agreement with the results in Figure 4.

As a further experiment,  $\text{NO}$ -rich feed gas ( $\text{NO}$ : 285 ppm;  $\text{NO}_2$ : 15 ppm) and  $\text{NO}_2$ -rich feed gas ( $\text{NO}$ : 45 ppm;  $\text{NO}_2$ : 255 ppm) were separately treated with acetaldehyde and n-heptane as a reducing agent, and the results are given in Figure 6. When n-heptane was used as a reducing agent, the  $\text{NO}_x$  conversion of the  $\text{NO}$ -rich feed gas was shown to be better than that of  $\text{NO}_2$ -rich feed gas, as in Figure 2. Similarly, it is clear in Figure 6 that even if acetaldehyde is used as a reducing agent,  $\text{NO}$ -rich feed gas is more easily reduced than  $\text{NO}_2$ -rich feed gas. With acetaldehyde, the  $\text{NO}_x$  conversions at 200 °C were 61.5% and 21% for the  $\text{NO}$ -rich and  $\text{NO}_2$ -rich feed gas, respectively, exhibiting about 40% difference in the  $\text{NO}_x$  conversion. At 250 °C, the difference in the  $\text{NO}_x$  conversion was also substantial; the  $\text{NO}_x$  conversions for the  $\text{NO}$ -rich and  $\text{NO}_2$ -rich feed gas were 99% and 68%, respectively. When the reaction temperature was further increased, the difference in the  $\text{NO}_x$  conversion between the  $\text{NO}$ -rich and  $\text{NO}_2$ -rich feed gas became negligible. In the case of  $\text{NH}_3$ -SCR, it has been reported that the best catalytic activity can be achieved by adjusting the  $\text{NO}/\text{NO}_2$  ratio to around 1/1 [13,14]. Unlike  $\text{NH}_3$ -SCR,

however, the formation of  $\text{NO}_2$  in HC-SCR had a negative effect on the  $\text{NO}_x$  reduction, even with equal amounts of  $\text{NO}$  and  $\text{NO}_2$  (see Figure 2). The results in Figure 6 show again that the improvement of HC-SCR performance by plasma is not due to the formation of  $\text{NO}_2$ .

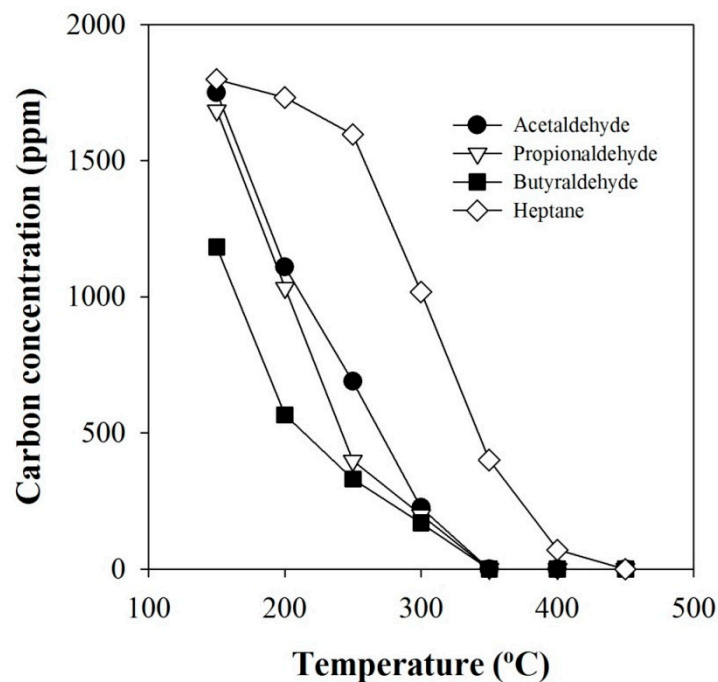


**Figure 5.** Concentrations of remaining aldehydes and n-heptane after the catalytic reactions without plasma ( $C_1/\text{NO}_x$ : 6).

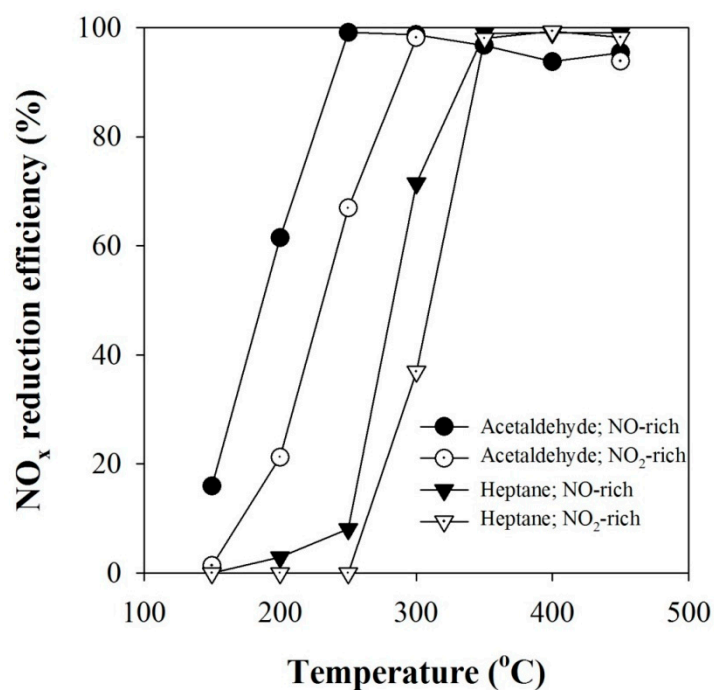


**Figure 6.** Comparison of the  $\text{NO}_x$  conversions between the  $\text{NO}$ -rich feed gas and  $\text{NO}_2$ -rich feed gas for the acetaldehyde and n-heptane reducing agents.

### 3. Experimental Section

#### 3.1. Materials

The catalyst Ag/ $\gamma$ -Al<sub>2</sub>O<sub>3</sub> was prepared by mixing 20-nm Ag nanoparticles (CNVISON Co., Ltd., Seoul, Korea) and  $\gamma$ -Al<sub>2</sub>O<sub>3</sub> support (specific surface area: 175 m<sup>2</sup> g<sup>-1</sup>; Alfa Aesar, Ward Hill, MA, USA). The mixture was well-blended so that the Ag nanoparticles were uniformly dispersed. The Ag loading in the prepared catalyst was 2 wt %. Previous studies reported that silver supported on  $\gamma$ -alumina exhibited high catalytic activity in the hydrocarbon SCR process [37,38]. The Ag-loaded  $\gamma$ -Al<sub>2</sub>O<sub>3</sub> was dried overnight at 110 °C to drive off water, and then a thermal treatment was performed at 550 °C for 6 h to remove any possible impurities. After the thermal treatment, pelletizing, crushing and sieving were performed. Only the granules having a size of 1.18–3.35 mm were selected and used as the catalyst. Figure 7 shows transmission electron microscope (TEM, JEM-2100F, JEOL, Tokyo, Japan) images of the 20-nm Ag nanoparticles and the prepared catalyst. The analysis by means of a surface area and pore size analyzer (Autosorb-1-mp, Quantachrome Instruments, Boynton Beach, FL, USA) showed that the pore of the catalyst was in the form of a cylinder, a typical IV shape defined by IUPAC. Miessner et al. [29] reported that the pore size distribution is an important factor in the catalytic activity, and pore and pore size distributions below 5 nm are essential for the SCR process. The average pore size of the prepared catalyst was ~3 nm (pore volume: 0.45 cc g<sup>-1</sup>), and confirmed to be suitable for the SCR process.

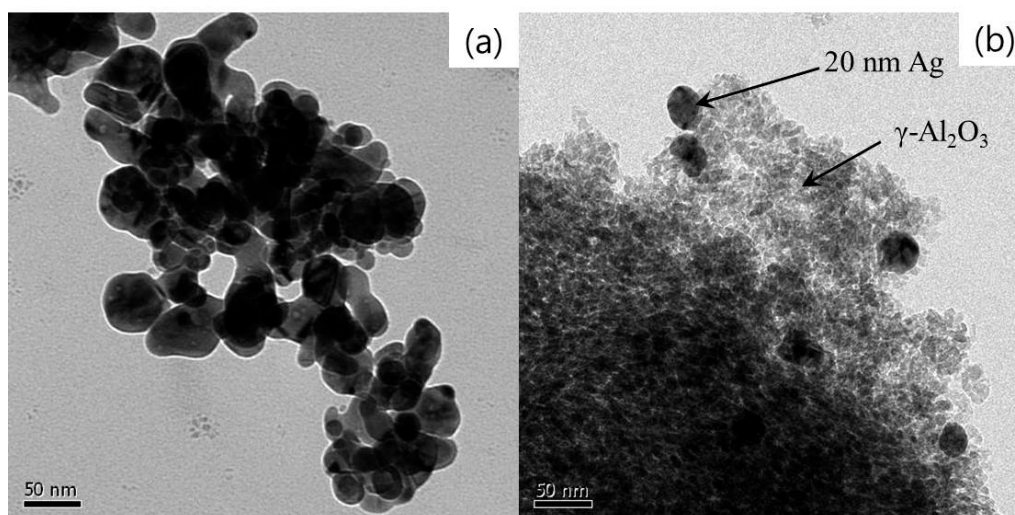


**Figure 7.** TEM images of (a) the 20-nm Ag nanoparticles and (b) the prepared Ag/ $\gamma$ -Al<sub>2</sub>O<sub>3</sub> catalyst.

#### 3.2. Methods

Figure 8 shows the schematic diagram of the plasma-coupled SCR reactor system. The plasma-SCR reactor is composed of a quartz tube having an inner diameter of 17.5 mm (thickness: 1.5 mm) and a discharging electrode (3.5 mm stainless steel) inserted coaxially in the center of the quartz tube. An aluminum foil (length: 5 cm) was wrapped around the quartz tube and used as the ground electrode. When an alternating current (AC) high voltage is applied between the discharging and ground electrode, plasma is generated inside the quartz tube. Plasma is created only in the area wrapped by the aluminum foil. The catalyst pellets were packed in the plasma generation region, and the filling length was 5 cm (8.8 g; 11.5 cm<sup>3</sup>). Quartz wool was used to fix the catalyst bed at both ends. The plasma-SCR reactor was installed in a furnace (DTF-50300, Daeheung Science Co., Incheon, Korea) equipped with a proportional-integral controller (PID controller) to control the reaction temperature.

The total flow rate of the feed gas injected into the plasma-SCR reactor was  $2 \text{ L min}^{-1}$  (space velocity:  $10,400 \text{ h}^{-1}$ ). The feed gas consisted of  $\text{N}_2$  (87.3%),  $\text{O}_2$  (9.7%),  $\text{H}_2\text{O}$  (3%) and  $\text{NO}$  (300 ppm). The flow rate of each gas was precisely controlled by a mass flow controller (MFC-500, Atovac Co., Yongin, Korea). The reducing agent, i.e., n-heptane (Sigma-Aldrich, St. Louis, MO, USA) was injected at the desired concentration by using its vapor pressure. As depicted in Figure 8, a porous gas diffuser was immersed in a bottle containing n-heptane and nitrogen gas was flowed through the diffuser to be saturated with n-heptane. The nitrogen saturated with n-heptane was mixed with  $\text{N}_2$ ,  $\text{O}_2$ ,  $\text{H}_2\text{O}$  and  $\text{NO}$ . The concentration of n-heptane is determined by the flow rate of nitrogen flowing through the diffuser. To keep the vapor pressure of n-heptane constant during the experiment, the bottle containing n-heptane was maintained at  $10^\circ\text{C}$  using a water bath. The concentration of n-heptane was six times the  $\text{NO}_x$  concentration on a  $\text{C}_1$  basis. In our previous work [39], it has been found that the optimum  $\text{C}_1/\text{NO}_x$  ratio is 6. Bao et al. [33] also reported that the highest  $\text{NO}_x$  conversion efficiency of HC-SCR was achieved at a  $\text{C}_1/\text{NO}_x$  ratio of 6–7. The method of injecting water vapor using the vapor pressure was the same as that of injecting n-heptane. The bottle containing distilled water was maintained at  $25^\circ\text{C}$ .

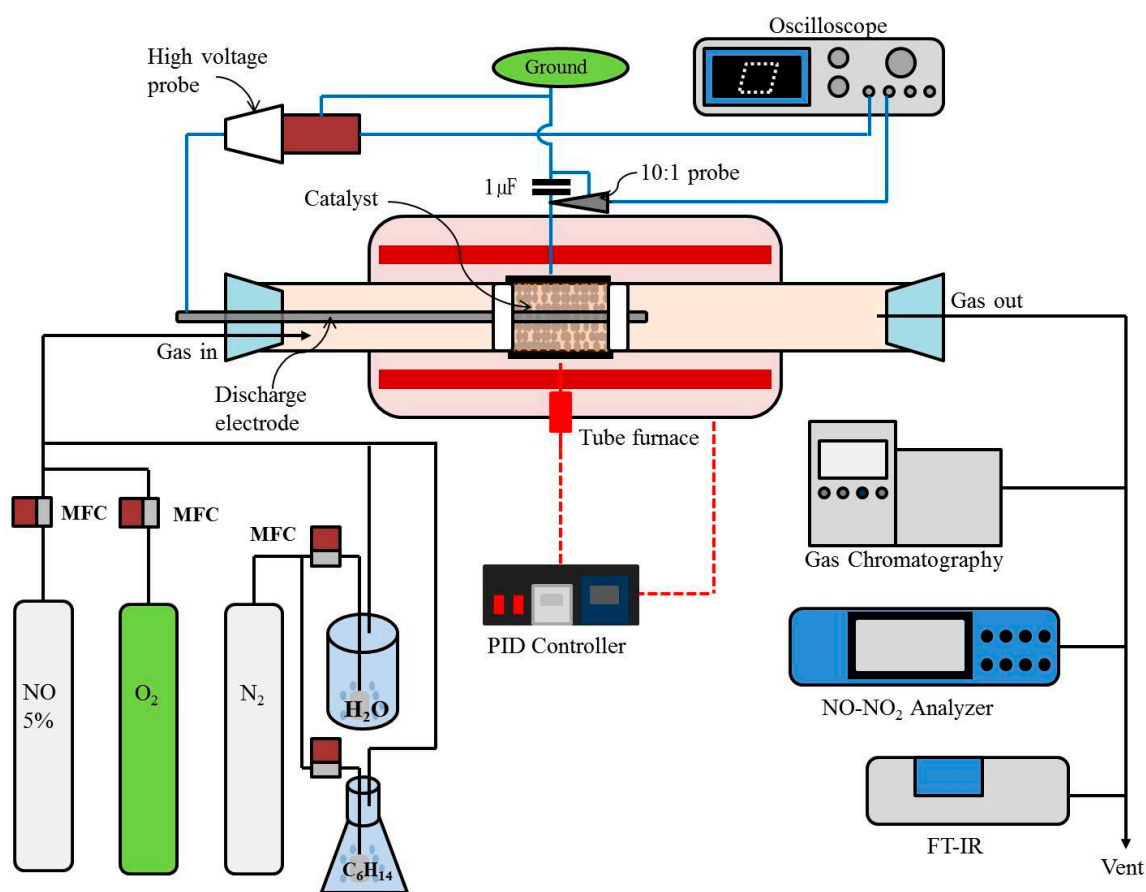


**Figure 8.** Schematic diagram of the plasma-coupled HC-SCR reactor system.

The electric power delivered to the plasma-SCR reactor was changed by varying the voltage applied between the discharging and ground electrode (operating frequency: 60 Hz). The power dissipated in the plasma-SCR reactor was determined by the Lissajous charge-voltage figure [19]. A capacitor was connected in series to the plasma-SCR reactor to measure the charge. The voltages across the electrodes of the plasma-SCR reactor and the capacitor were measured with a 1000:1 high-voltage probe (Probe P6015, Tektronix, Beaverton, OR, USA) and a 10:1 voltage probe (P69139, Tektronix, Beaverton, OR, USA), respectively. The measured voltages were recorded on a digital

oscilloscope (TDS 3034, Tektronix, Beaverton, OR, USA). Figure 9 shows photos of the plasma discharge taken by increasing the applied voltage from 11 to 25 kV. At lower voltages, the plasma was created near the discharging electrode and inner wall of the quartz tube. At higher voltages, the plasma covered the whole catalyst bed, but the plasma created near the discharging electrode and inner wall of the quartz tube was still intense.

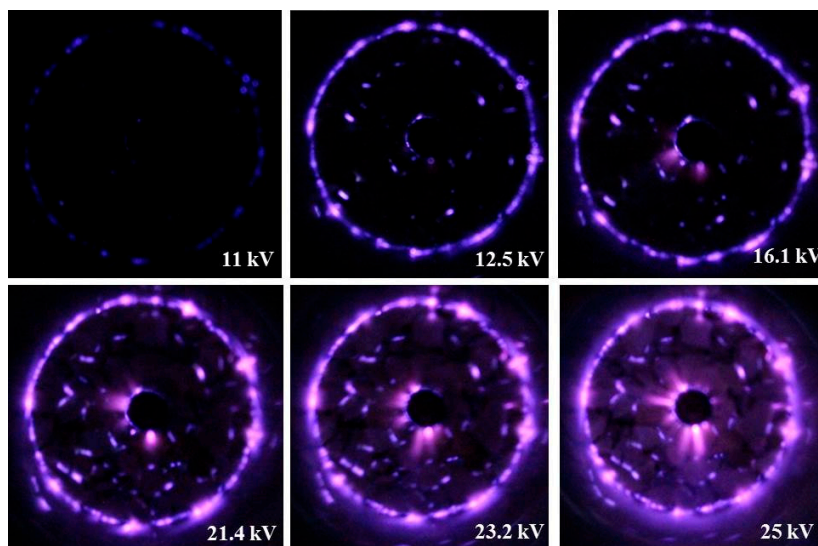


**Figure 9.** Photos of the plasma discharge at different voltages from 11 to 25 kV.

The energy consumed in the plasma–catalytic reactor depends on the discharge voltage. In order to estimate the energy consumption of the plasma–catalytic reactor, the specific input energy (SIE) was calculated based on the discharge power in Figure 1a as follows:

$$SIE \text{ (J/L)} = \frac{P \text{ (W)}}{Q \text{ (L/s)}} \quad (8)$$

where  $P$  is discharge power, and  $Q$  is gas flow rate. For information, the gas flow rate of  $2 \text{ L min}^{-1}$  is equivalent to  $0.0333 \text{ L s}^{-1}$ . The relation between the value of SIE and the discharge voltage is shown in Figure 10.

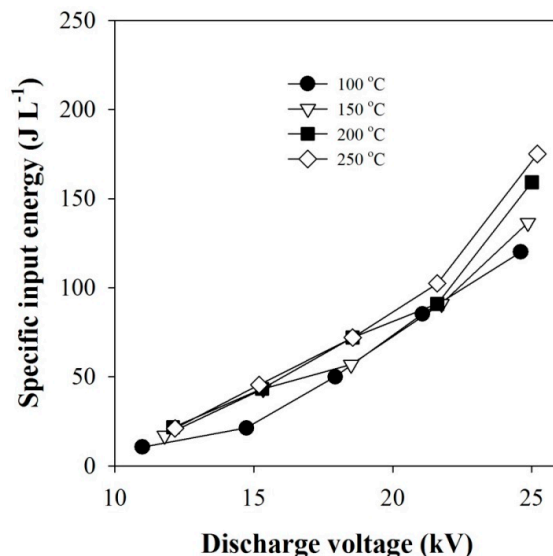


Figure 10. Effect of discharge voltage on the specific input energy.

The concentrations of NO and NO<sub>2</sub> were analyzed using a NO-NO<sub>2</sub> analyzer (rbr-Computertechnik GmbH, DE/dcom-KD, Iserlohn, Germany). A Fourier transform infrared spectrophotometer (FTIR-7600, Lambda Scientific, Edwardstown, Australia) was used to analyze the concentrations of n-heptane, CO and CO<sub>2</sub>. The resolution of FTIR was set to 1 cm<sup>-1</sup>, and the number of measurement iterations was set to 10. The path length of the infrared gas cell was 16 cm and the window material was CaF<sub>2</sub>. The decomposition products of n-heptane were identified and quantified by a gas chromatograph (Bruker 450-GC, Fitchburg, WI, USA) equipped with a flame ionization detector (FID) and a 60-m long capillary column (BR-624ms, Bruker, Fitchburg, WI, USA). The concentration of ammonia was measured using a chemical detector tube (Product No. 3L; Measuring range 0.5–78 ppm; Gastec Co., Tokyo, Japan).

#### 4. Conclusions

In the present catalytic NO<sub>x</sub> reduction system with Ag/γ-Al<sub>2</sub>O<sub>3</sub>, the NO<sub>x</sub> conversion was improved by 30–80%, depending on whether plasma was generated in the catalyst bed or not. This work focused on identifying the role of plasma and understanding the mechanisms involved in the plasma-enhanced HC-SCR. In the plasma-coupled catalytic system, plasma readily oxidized NO to NO<sub>2</sub> and decomposed the hydrocarbon reducing agent. Unlike NH<sub>3</sub>-SCR, the formation of NO<sub>2</sub> in HC-SCR was found to negatively affect the conversion of NO<sub>x</sub>, and the main cause of plasma-enhanced NO<sub>x</sub> conversion was the formation of oxygenated hydrocarbons such as acetaldehyde, propionaldehyde and butyraldehyde. Through several sets of experiments carried out by injecting each aldehyde separately as a reducing agent, it was shown that the aldehydes had much higher NO<sub>x</sub> reduction capability than n-heptane. Particularly, the more the number of carbons in the aldehyde molecule, the higher the NO<sub>x</sub> conversion was. Thus, it can be concluded that the main role of plasma in the HC-SCR is to produce oxygenated compounds with better reducing capability.

**Supplementary Materials:** The following are available online at [www.mdpi.com/2073-4344/7/11/325/s1](http://www.mdpi.com/2073-4344/7/11/325/s1), Figure S1: Typical FTIR spectrum of the effluent obtained at a voltage of 18 kV (the inset shows the N<sub>2</sub>O concentration as a function of discharge voltage), Figure S2: NO and NO<sub>2</sub> concentrations at the reactor outlet as a function of discharge voltage, Figure S3: Concentrations of n-heptane decomposition products such as acetaldehyde, propionaldehyde and butyraldehyde as a function of discharge voltage.

**Acknowledgments:** This work was supported by the Basic Science Research Program through the National Research Foundation funded by the Ministry of Science, ICT and Future Planning, Korea (Grant No. 2016R1A2A2A05920703).

**Author Contributions:** Byeong Ju Lee, Ho-Chul Kang and Jin Oh Jo carried out the experimental work and analyzed the data; Young Sun Mok supervised all the study.

**Conflicts of Interest:** The authors declare no conflict of interest.

## References

1. Jacobson, M.Z. *Air Pollution and Global Warming: History, Science, and Solutions*, 2nd ed.; Stanford University: Stanford, CA, USA, 2012; ISBN 9781107691155.
2. Schill, L.; Putluru, S.S.R.; Fehrmann, R.; Jensen, A.D. Low-temperature NH<sub>3</sub>-SCR of NO on mesoporous Mn<sub>0.6</sub>Fe<sub>0.4</sub>/TiO<sub>2</sub> prepared by a hydrothermal method. *Catal. Lett.* **2014**, *144*, 395–402. [[CrossRef](#)]
3. Cheng, X.; Bi, X.T. A review of recent advances in selective catalytic NO<sub>x</sub> reduction reactor technologies. *Particuology* **2014**, *16*, 1–18. [[CrossRef](#)]
4. Brandenberger, S.; Krocher, O.; Casapu, M.; Tissler, A.; Althoff, R. Hydrothermal deactivation of Fe-ZSM-5 catalysts for the selective catalytic reduction of NO with NH<sub>3</sub>. *Appl. Catal. B Environ.* **2011**, *101*, 649–659. [[CrossRef](#)]
5. Metkar, P.S.; Harold, M.P.; Balakotaiah, V. Experimental and kinetic modeling study of NH<sub>3</sub>-SCR of NO<sub>x</sub> on Fe-ZSM-5, Cu-chabazite and combined Fe- and Cu-zeolite monolithic catalysts. *Chem. Eng. Sci.* **2013**, *87*, 51–66. [[CrossRef](#)]
6. Eranen, K.; Lindfors, L.E.; Klingstedt, F.; Murzin, D.Y. Continuous reduction of NO with octane over a silver/alumina catalyst in oxygen-rich exhaust gases: Combined heterogeneous and surface-mediated homogeneous reactions. *J. Catal.* **2003**, *219*, 25–40. [[CrossRef](#)]
7. Kim, Y.J.; Kwon, H.J.; Heo, I.; Nam, I.-S.; Cho, B.K.; Choung, J.W.; Cha, M.-S.; Yeo, G.K. Mn-Fe/ZSM5 as a low-temperature SCR catalyst to remove NO<sub>x</sub> from diesel engine exhaust. *Appl. Catal. B Environ.* **2012**, *126*, 9–21. [[CrossRef](#)]
8. Yang, T.T.; Bi, H.T.; Cheng, X.X. Effects of O<sub>2</sub>, CO<sub>2</sub> and H<sub>2</sub>O on NO<sub>x</sub> adsorption and selective catalytic reduction over Fe/ZSM-5. *Appl. Catal. B Environ.* **2011**, *102*, 163–171. [[CrossRef](#)]
9. Zhang, L.; Sha, X.-L.; Zhang, L.; He, H.; Ma, Z.; Wang, L.; Wang, Y.; She, L. Synergistic catalytic removal NO<sub>x</sub> and the mechanism of plasma and hydrocarbon gas. *AIP Adv.* **2016**, *6*. [[CrossRef](#)]
10. Lee, T.Y.; Bai, H. Low temperature selective catalytic reduction of NO<sub>x</sub> with NH<sub>3</sub> over Mn-based catalyst: A review. *AIMS Environ. Sci.* **2016**, *3*, 261–289. [[CrossRef](#)]
11. Ciardelli, C.; Nova, I.; Tronconi, E.; Chatterjee, D.; Bandl-Konrad, B. A “nitrate route” for the low temperature “fast SCR” reaction over a V<sub>2</sub>O<sub>5</sub>-WO<sub>3</sub>/TiO<sub>2</sub> commercial catalyst. *Chem. Commun.* **2004**, *23*, 2718–2719. [[CrossRef](#)] [[PubMed](#)]
12. Iwasaki, M.; Shinjoh, H. A comparative study of “standard”, “fast” and “NO<sub>2</sub>” SCR reactions over Fe/zeolite catalyst. *Appl. Catal. A Gen.* **2010**, *390*, 71–77. [[CrossRef](#)]
13. Koebel, M.; Madia, G.; Elsener, M. Selective catalytic reduction of NO and NO<sub>2</sub> at low temperatures. *Catal. Today* **2002**, *73*, 239–247. [[CrossRef](#)]
14. Grossale, A.; Nova, I.; Tronconi, E.; Chatterjee, D.; Weibel, M. The chemistry of the NO/NO<sub>2</sub>-NH<sub>3</sub> “fast” SCR reaction over Fe-ZSM5 investigated by transient reaction analysis. *J. Catal.* **2008**, *256*, 312–322. [[CrossRef](#)]
15. Piumetti, M.; Bensaid, S.; Fino, D.; Russo, N. Catalysis in diesel engine NO<sub>x</sub> after treatment: A review. *Catal. Struct. React.* **2015**, *1*, 155–173. [[CrossRef](#)]
16. Tonkyn, R.G.; Barlowa, S.E.; Hoard, J.W. Reduction of NO<sub>x</sub> in synthetic diesel exhaust via two-step plasma-catalysis treatment. *Appl. Catal. B Environ.* **2003**, *40*, 207–217. [[CrossRef](#)]
17. Pan, H.; Guo, Y.; Jian, Y.; He, C. Synergistic effect of non-thermal plasma on NO<sub>x</sub> Reduction by CH<sub>4</sub> over an In/H-BEA catalyst at low temperatures. *Energy Fuels* **2015**, *29*, 5282–5289. [[CrossRef](#)]
18. Chen, H.L.; Lee, H.M.; Chen, S.H.; Chang, M.B.; Yu, S.J.; Li, S.N. Removal of volatile organic compounds by single-stage and two-stage plasma catalysis systems: A review of the performance enhancement mechanisms, current status, and suitable applications. *Environ. Sci. Technol.* **2009**, *43*, 2216–2227. [[CrossRef](#)] [[PubMed](#)]
19. Trinh, Q.H.; Mok, Y.S. Environmental plasma-catalysis for the energy-efficient treatment of volatile organic compounds. *Korean J. Chem. Eng.* **2016**, *33*, 735–748. [[CrossRef](#)]
20. Whitehead, J.C. Plasma-catalysis: The known knowns, the known unknowns and the unknown unknowns. *J. Phys. D Appl. Phys.* **2016**, *49*, 243001. [[CrossRef](#)]
21. Stere, C.E.; Adress, W.; Burch, R.; Chansai, S.; Goguet, A.; Graham, W.G.; De Rosa, F.; Palma, V.; Hardacre, C. Ambient temperature hydrocarbon selective catalytic reduction of NO<sub>x</sub> using atmospheric pressure non-thermal plasma activation of a Ag/Al<sub>2</sub>O<sub>3</sub> catalyst. *ACS Catal.* **2014**, *4*, 666–673. [[CrossRef](#)]

22. Yu, Q.; Liu, T.; Wang, H.; Xiao, L.; Chen, M.; Jiang, X.; Zheng, X. Cold plasma-assisted selective catalytic reduction of NO over B<sub>2</sub>O<sub>3</sub>/γ-Al<sub>2</sub>O<sub>3</sub>. *Chin. J. Catal.* **2012**, *33*, 783–789. [[CrossRef](#)]
23. Jiang, N.; Shang, K.-F.; Lu, N.; Li, H.; Li, J.; Wu, Y. High-efficiency removal of NO<sub>x</sub> from flue gas by multitooth wheel-cylinder corona discharge plasma facilitated selective catalytic reduction process. *IEEE Trans. Plasma Sci.* **2016**, *44*, 2738–2744. [[CrossRef](#)]
24. Guan, B.; Lin, H.; Cheng, Q.; Huang, Z. Removal of NO<sub>x</sub> with selective catalytic reduction based on nonthermal plasma preoxidation. *Ind. Eng. Chem. Res.* **2011**, *50*, 5401–5413. [[CrossRef](#)]
25. Talebizadeh, P.; Babaie, M.; Brown, R.; Rahimzadeh, H.; Ristovski, Z.; Arai, M. The role of non-thermal plasma technique in NO<sub>x</sub> treatment: A review. *Renew. Sustain. Energy Rev.* **2014**, *40*, 886–901. [[CrossRef](#)]
26. Wang, J.; He, T.; Li, C. Majorization of working parameters for non-thermal plasma reactor and impact on no oxidation of diesel engine. *Int. J. Automot. Technol.* **2017**, *18*, 229–233. [[CrossRef](#)]
27. Pan, H.; Qiang, Y. Promotion of non-thermal plasma on catalytic reduction of NO<sub>x</sub> by C<sub>3</sub>H<sub>8</sub> over Co/BEA catalyst at low temperature. *Plasma Chem. Plasma Process.* **2014**, *34*, 811–824. [[CrossRef](#)]
28. Cho, B.K.; Lee, J.-H.; Crellin, C.C.; Olson, K.L.; Hilden, D.L.; Kim, M.K.; Kim, P.S.; Heo, I.; Oh, S.H.; Nam, I.-S. Selective catalytic reduction of NO<sub>x</sub> by diesel fuel: Plasma-assisted HC/SCR system. *Catal. Today* **2012**, *191*, 20–24. [[CrossRef](#)]
29. Miessner, H.; Francke, K.; Rudolph, R. Plasma-enhanced HC-SCR of NO<sub>x</sub> in the presence of excess oxygen. *Appl. Catal. B Environ.* **2002**, *36*, 53–62. [[CrossRef](#)]
30. Mok, Y.S.; Nam, I.-S. Reduction of nitrogen oxides by ozonization-catalysis hybrid process. *Korean J. Chem. Eng.* **2004**, *21*, 976–982. [[CrossRef](#)]
31. Jogi, I.; Stamate, E.; Irimiea, C.; Schmidt, M.; Brandenburg, R.; Hołub, M.; Bonisławski, M.; Jakubowski, T.; Kaariainen, M.-L.; Cameron, D.C. Comparison of direct and indirect plasma oxidation of NO combined with oxidation by catalyst. *Fuel* **2015**, *144*, 137–144. [[CrossRef](#)]
32. Jogi, I.; Levoll, E.; Raud, J. Plasma oxidation of NO in O<sub>2</sub>:N<sub>2</sub> mixtures: The importance of back-reaction. *Chem. Eng. J.* **2016**, *301*, 149–157. [[CrossRef](#)]
33. Bao, X.Y.; Malik, M.A.; Norton, D.G.; Neculaes, V.B.; Schoenbach, K.H.; Heller, R.; Siclovan, O.P.; Corah, S.E.; Caiafa, A.; Inzinna, L.P.; et al. Shielded sliding discharge-assisted hydrocarbon selective catalytic reduction of NO<sub>x</sub> over Ag/Al<sub>2</sub>O<sub>3</sub> catalysts using diesel as a reductant. *Plasma Chem. Plasma Process.* **2014**, *34*, 825–836. [[CrossRef](#)]
34. Mhadeshwar, A.B.; Winkler, B.H.; Eiteneer, B.; Hancu, D. Microkinetic modeling for hydrocarbon (HC)-based selective catalytic reduction (SCR) of NO<sub>x</sub> on a silver-based catalyst. *Appl. Catal. B Environ.* **2009**, *89*, 229–238. [[CrossRef](#)]
35. Gao, X.; Yu, Q.; Chen, L. Selective catalytic reduction of NO with methane. *J. Nat. Gas Chem.* **2003**, *12*, 264–270.
36. Yeom, Y.H.; Li, M.; Sachtler, W.M.H.; Weitz, E. A study of the mechanism for NO<sub>x</sub> reduction with ethanol on γ-alumina supported silver. *J. Catal.* **2006**, *238*, 100–110. [[CrossRef](#)]
37. Furusawa, T.; Seshan, K.; Lercher, J.A.; Lefferts, L.; Aika, K. Selective reduction of NO to N<sub>2</sub> in the presence of oxygen over supported silver catalysts. *Appl. Catal. B Environ.* **2002**, *37*, 205–216. [[CrossRef](#)]
38. He, H.; Li, Y.; Zhang, X.; Yu, Y.; Zhang, C. Precipitable silver compound catalysts for the selective catalytic reduction of NO<sub>x</sub> by ethanol. *Appl. Catal. A Gen.* **2010**, *375*, 258–264. [[CrossRef](#)]
39. Ihm, T.H.; Jo, J.O.; Hyun, Y.J.; Mok, Y.S. Removal of nitrogen oxides using hydrocarbon selective catalytic reduction coupled with plasma. *Appl. Chem. Eng.* **2016**, *27*, 92–100. [[CrossRef](#)]

